Electronic Supplementary Information

Mitigation of Jahn-Teller Distortion and Na^+/Vacancy Ordering in P′2-$Na_{0.67}MnO_2$ Cathode Material by Li Substitution

Yanchen Liu, Chenchen Wang, Shuo Zhao, Lin Zhang, Kai Zhang, Fujun Li,* and Jun Chen

Key Laboratory of Advanced Energy Materials Chemistry (Ministry of Education), College of Chemistry, Nankai University, Tianjin 300071, P.R.China

E-mail: fujunli@nankai.edu.cn

Experimental Section

Materials synthesis: P′2-$Na_{0.67}Li_xMn_{1-x}O_2$ (x = 0, 0.03, 0.05 and 0.08) were prepared by a facile solid-state method. Stoichiometric Na_2CO_3 (5 mol% excess), Li_2CO_3 (5 mol% excess) and Mn_2O_3 were ball milled with acetone at 400 rpm for 12 h. The mixtures were dried and pressed into pellets. The precursors were heated in air atmosphere at 1000 ^oC for 15 h, then quenched to room temperature, and transferred to an argon-filled glove box until use.

Materials characterization: The crystal structure of the materials was characterized with a X-ray diffractometer (Rigaku SmartLab) using Cu Kα radiation. Rietveld refinement was carried out using general structure analysis system (GSAS-II). ICP-OES (SpectroBlue) was conducted to analyze the compositions of materials. Solid-state ^7Li NMR spectra were obtained on a JNM-ECZ600R widebore spectrometer. XPS measurements were performed on a Perkin Elmer PHI 1600 ESCA system. SEM (JEOL JSM-7500F) and TEM (FEI, Talos F200X G2, AEMC) were employed to record the morphologies and crystal structure. SIMS was examined on a Cameca IMS-5FE7 system using Cs^+ primary ions with a beam current of 3 nA. The analysis area of samples is 33 μm in diameter and the raster is 16 μm.

Electrochemical measurements: The electrochemical tests were carried out in coin cells (CR2032), which were assembled in an argon-filled glove box ($O_2 \leq$ 0.1 ppm, $H_2O \leq$ 0.1 ppm). The electrode was prepared by mixing active material, Super P carbon and poly(vinyl difluride) (PVDF) in a weight ratio of 8:1:1 onto aluminum foil, followed by drying at 80 °C in vacuum for 12h. The loading mass of active material was about 1.5~2.0 mg cm^{-2}. Sodium foil was used as negative electrode, and glass fiber was used as separator. The electrolyte was $NaPF_6$ in the propylene carbonate (PC) with 2 wt% fluoroethylene carbonate (FEC). CV was carried out at a scan rate of 0.1 mV s^{-1} on a Solartron 1470 electrochemical work station. The charge and discharge tests and GITT were performed on a Land CT2001A battery-testing instrument. In GITT measurements, the cells were charged at 10 mA g^{-1} for 1.5 h, followed by a rest time of 30 min. The diffusion coefficients of Na^+ could be calculated according to the equation:

$$D = \frac{4}{\Pi\tau}\left(\frac{m_B V_M}{M_B S}\right)^2 \left(\frac{\Delta E_s}{\Delta E_\tau}\right)^2 \quad (1)$$

where m_B and M_B are the mass of active material and molecular weight, respectively. V_m is the molar volume of active material, and S is the area of electrode. ΔE_s and ΔE_τ represent the change in the steady-state voltage after subtracting the IR drop and transient change in voltage. The

capacitive contributions were quantified via CV measurements at varied scan rates from 0.1 to 1.0 mV s^{-1} between 1.5 and 4.4 V. The relationship between peak current (i) and scan rate (v) can be described as follows:

$$i = av^b \quad (1)$$

$$\log(i) = b\log(v) + \log(a) \quad (2)$$

where b determines the sodiation and desodiation behaviors. If *b* equals to 1, the electrochemical system is dominated by capacitance; if *b* is 0.5, the process is controlled by Na^+ diffusion.[1,2] The contributions of capacitance can be quantitatively calculated by eq 3:

$$i = k_1v + k_2v^{0.5} \quad (3)$$

where k_1v and $k_2v^{0.5}$ represent the capacitance and Na^+ diffusion.

Computational methods: The density functional theory calculations were performed with Vienna ab initio Simulation Package (VASP)[3,4] with projector augmented wave potentials and Perdew-Becke-Ernzerhof (PBE) exchange-correlation.[5] The cutoff energy was set to 520 eV, and all the structures are fully relaxed until the remaining forces fell below 0.01 eV $Å^{-1}$. Gamma-centered k-meshes with a density of 8000 k-points were sampled for the Brillouin zone. The DFT + U method[6] was used to address the localization of the d-orbital of Mn with U-J value of 3.9 according to previous studies.[7] COHP calculations were performed using the Local-

Orbital Basis Suite Towards Electronic-Structure Reconstruction (LOBSTER) code.[8,9] The Na^+ cation activation barriers were calculated using the climbing image nudged elastic band (CINEB) method[10] for both P′2-$Na_{0.67}Li_{0.05}Mn_{0.95}O_2$ and P′2-$Na_{0.67}MnO_2$ with one vacancy generated for Na^+ diffusion. Four intermediates were considered between the first and the final images of one Na^+ diffusion. All the atoms were allowed to relax with lattice parameters fixed during CINEB calculation.

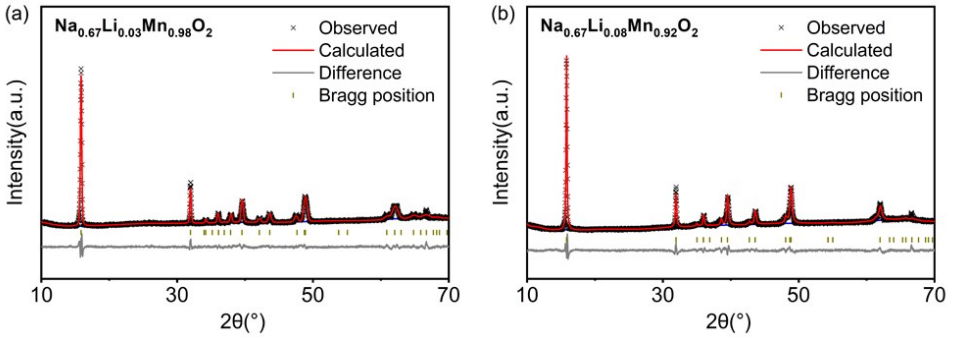

Fig. S1 Rietveld refinement of powder XRD data for (a) P′2-$Na_{0.67}Li_{0.03}Mn_{0.97}O_2$ and (b) P′2-$Na_{0.67}Li_{0.08}Mn_{0.92}O_2$.

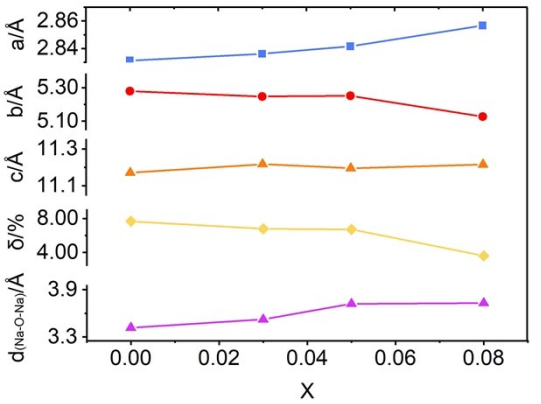

Fig. S2 Evolution of the lattice parameters, δ and Na interlayer space of P′2-$Na_{0.67}Li_xMn_{1-x}O_2$.

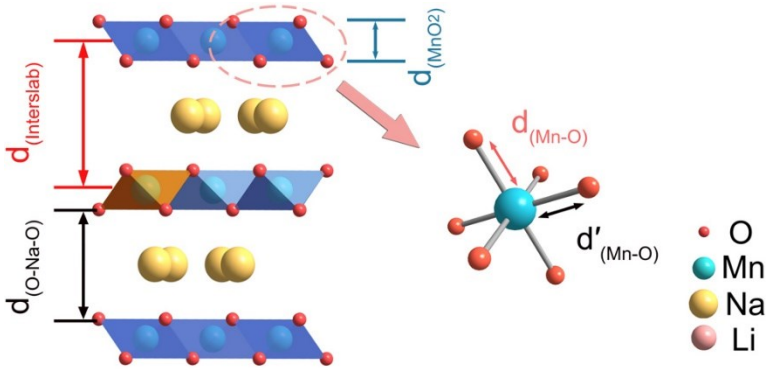

Fig. S3 Schematic illustration of P′2-$Na_{0.67}Li_xMn_{1-x}O_2$.

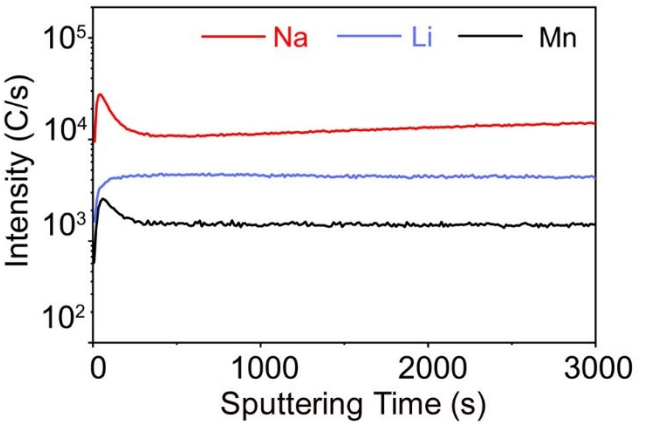

Fig. S4 Sputter depth profiles of P′2-$Na_{0.67}Li_{0.05}Mn_{0.95}O_2$.

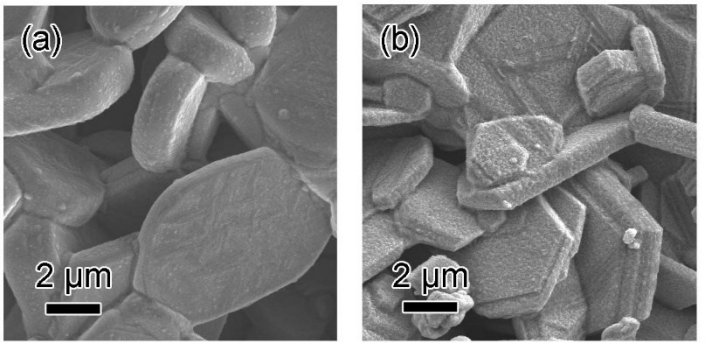

Fig. S5 SEM images of (a) P′2-$Na_{0.67}MnO_2$ and (b) P′2-$Na_{0.67}Mn_{0.95}Li_{0.05}O_2$-.

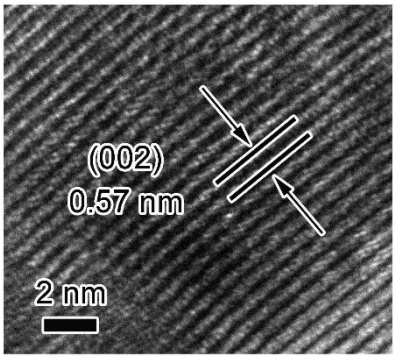

Fig. S6 HRTEM images of P′2-$Na_{0.67}MnO_2$.

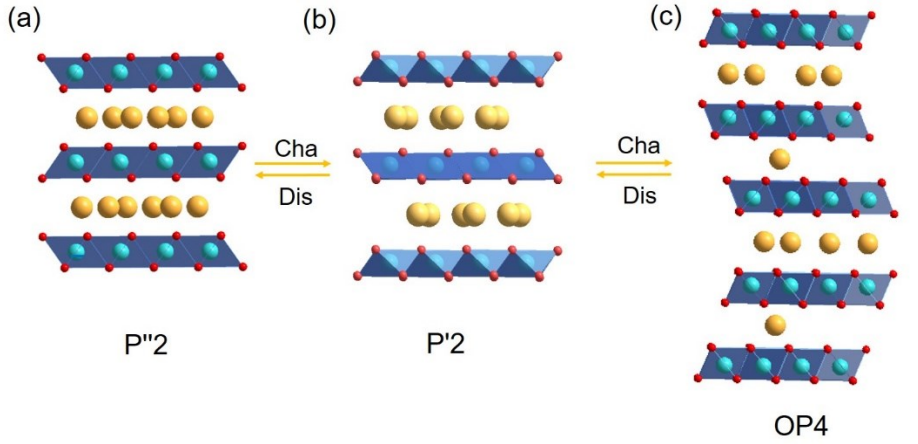

Fig. S7 Schematic illustration of (a) P"2-, (b) P'2- and (c) OP4-type phase.

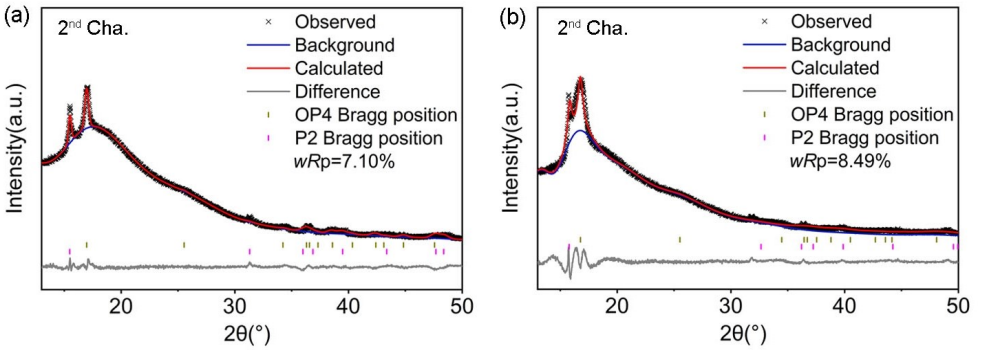

Fig. S8 Rietveld refinement of powder XRD data for (a) P′2-$Na_{0.67}MnO_2$ and (b) P′2-$Na_{0.67}Li_{0.05}Mn_{0.95}O_2$ electrode cycled at 4.3 V during second charge.

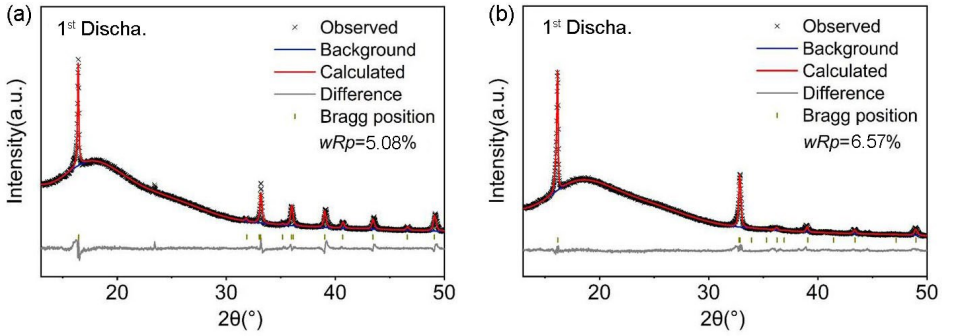

Fig. S9 Rietveld refinement of powder XRD data for (a) P′2-$Na_{0.67}MnO_2$ and (b) P′2-$Na_{0.67}Li_{0.05}Mn_{0.95}O_2$ electrode cycled at 1.8 V during first discharge.

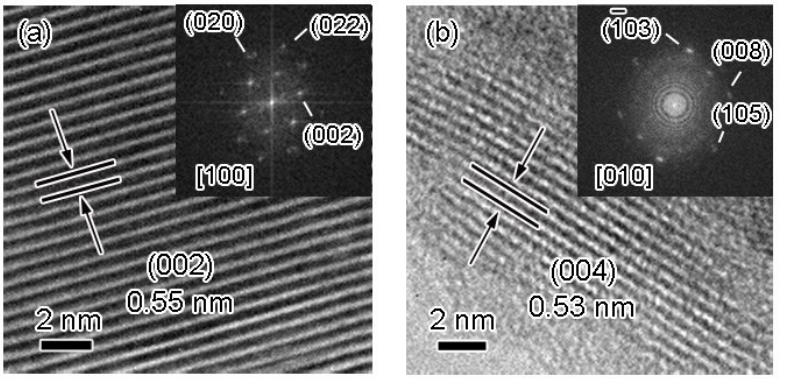

Fig. S10 HRTEM and FFT images of P′2-$Na_{0.67}Li_{0.05}Mn_{0.95}O_2$ electrodes: (a) fully discharged to 1.8 V and (b) fully charged to 4.3 V.

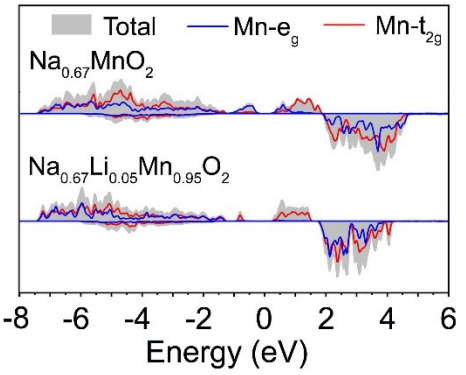

Fig. S11 Electronic density of states projected on Mn ion.

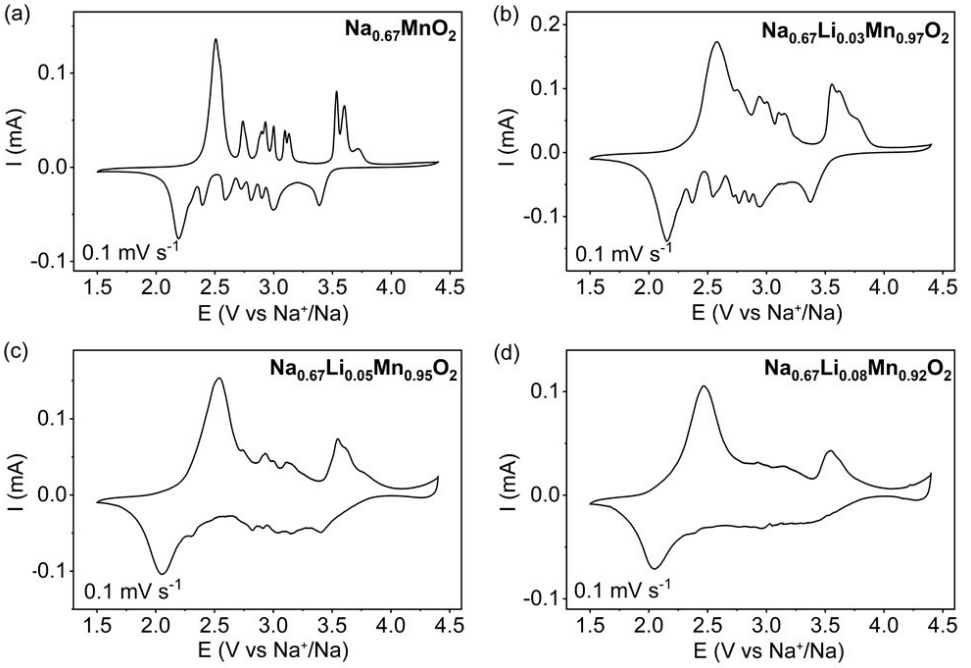

Fig. S12 Cyclic voltammograms of (a) $Na_{0.67}MnO_2$, (b) $Na_{0.67}Li_{0.03}Mn_{0.97}O_2$, (c) $Na_{0.67}Li_{0.05}Mn_{0.95}O_2$ and (d) $Na_{0.67}Li_{0.08}Mn_{0.92}O_2$ electrodes measured at a scan rate of 0.1 mV s^{-1} within 1.5-4.4 V.

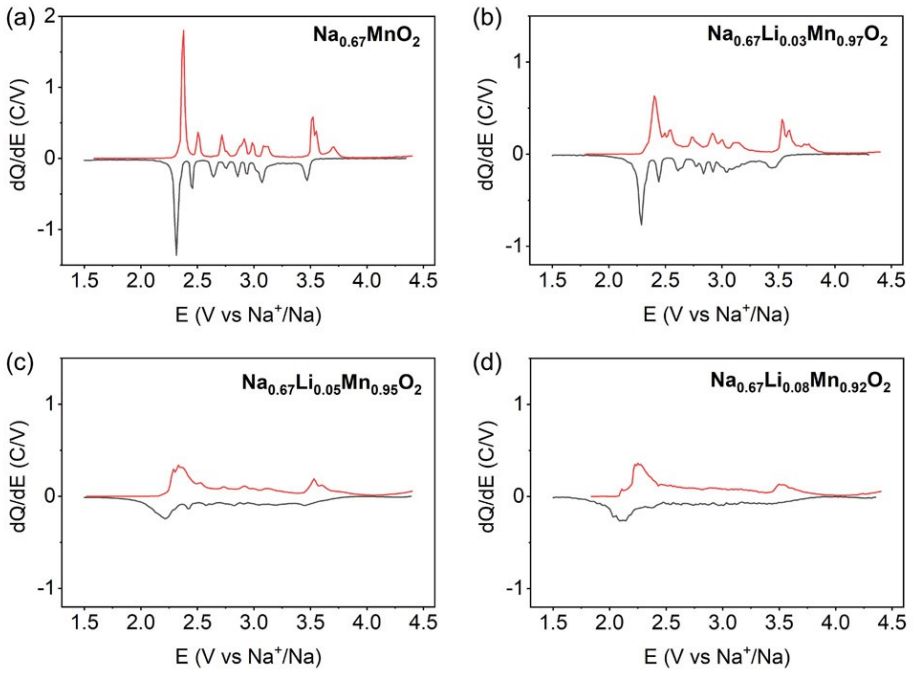

Fig. S13 dQ/dE curves of first discharge (bottom side) and second charge (upper side) of (a) $Na_{0.67}MnO_2$, (b) $Na_{0.67}Li_{0.03}Mn_{0.97}O_2$, (c) $Na_{0.67}Li_{0.05}Mn_{0.95}O_2$ and (d) $Na_{0.67}Li_{0.08}Mn_{0.92}O_2$ electrodes measured within 1.5-4.4 V.

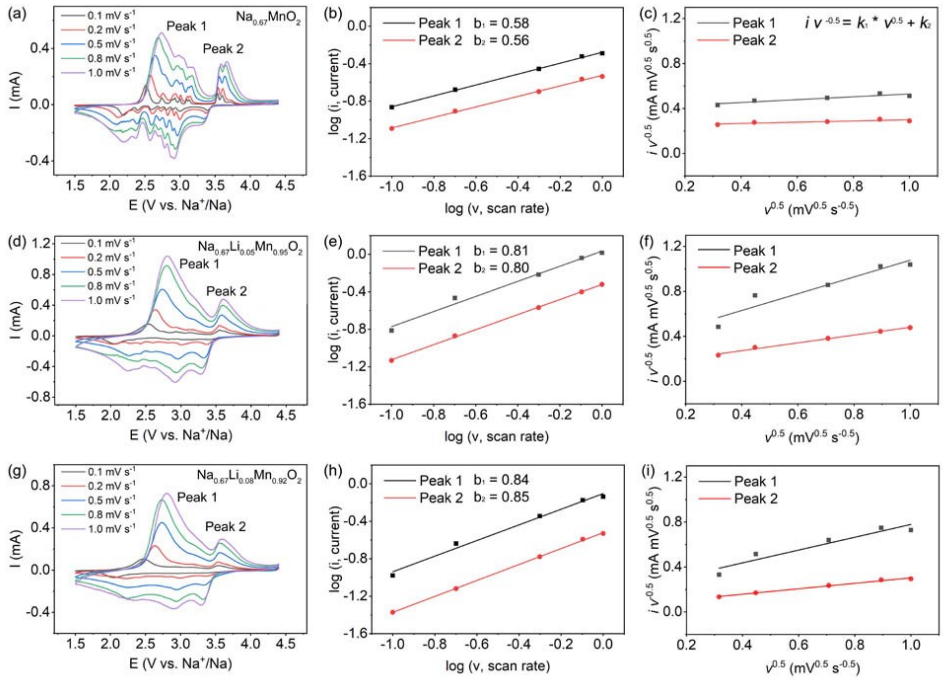

Fig. S14. CV profiles at different scan rates for (a) $Na_{0.67}MnO_2$, (d) $Na_{0.67}Li_{0.05}Mn_{0.95}O_2$ and (g) $Na_{0.67}Li_{0.08}Mn_{0.92}O_2$. Linear relationship of log(*i*) and log(*v*) of peak 1, 2 for (b) $Na_{0.67}MnO_2$, (e) $Na_{0.67}Li_{0.05}Mn_{0.95}O_2$ and (h) $Na_{0.67}Li_{0.08}Mn_{0.92}O_2$. Plots of $iv^{-0.5}$ against $v^{0.5}$ of peaks 1, 2 for (c) $Na_{0.67}MnO_2$, (f) $Na_{0.67}Li_{0.05}Mn_{0.95}O_2$ and (i) $Na_{0.67}Li_{0.08}Mn_{0.92}O_2$. The constants k_1 and k_2 can be used to evaluate the capacitive and Na^+ ion diffusion contribution, respectively.

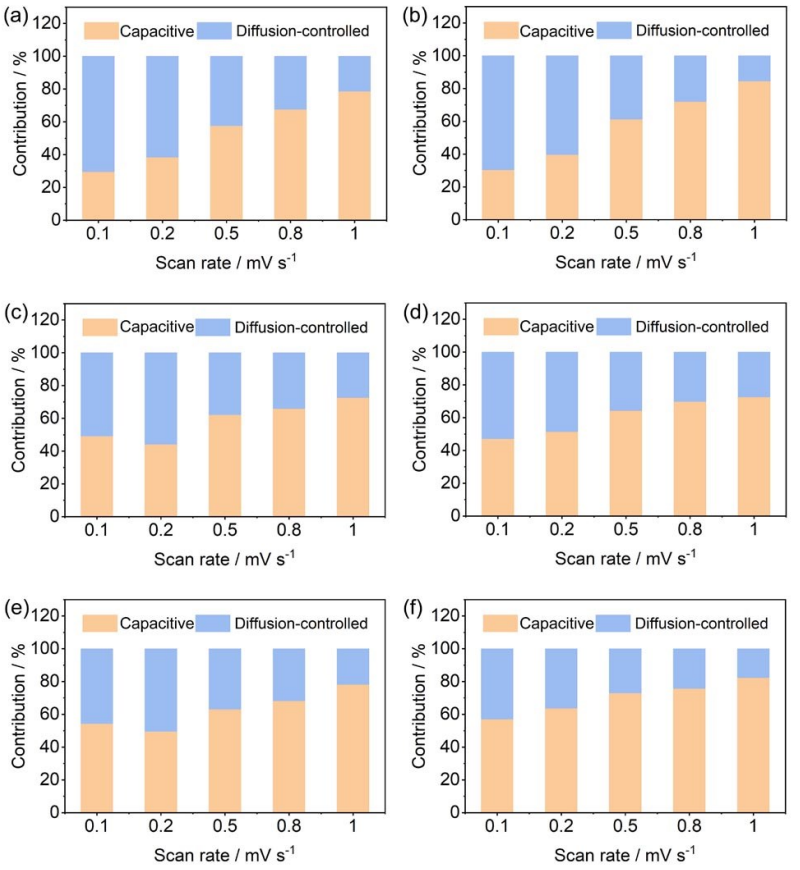

Fig. S15. Ratio of the capacitive and diffusion-controlled capacities at different scan rate for (a) peak 1 and (b) peak 2 of $Na_{0.67}MnO_2$; (c) peak 1 and (d) peak 2 of $Na_{0.67}Li_{0.05}Mn_{0.95}O_2$; (e) peak 1 and (f) peak 2 of $Na_{0.67}Li_{0.08}Mn_{0.92}O_2$.

Table S1. Rietveld refinement results for P′2-$Na_{0.67}MnO_2$.

Sample	Atom	Site	x	y	z	g	B_{iso}
$Na_{0.67}MnO_2$	Na_f	4c	0	-0.072	0.250	0.184	1.14
	Na_e	4c	0	0.312	0.250	0.475	2.40
	Mn	4a	0	0	0	1	0.53
	O	8f	0	0.652	0.097	1	4.52

Space group: *Cmcm*, a = 2.831 Å, b = 5.280 Å, c = 11.171 Å, α = β = γ= 90°, Vol = 166.993 Å^3, (Z = 4), *Rp* = 2.66%, R_{wp} = 4.07%， χ^2 = 6.554. g: occupancy. x, y, z: atomic coordinate.

Table S2. Rietveld refinement results for P′2-$Na_{0.67}Li_{0.03}Mn_{0.97}O_2$.

Sample	Atom	Site	x	y	z	g	B_{iso}
$Na_{0.67}Li_{0.03}Mn_{0.97}O_2$	Na_f	4c	0	-0.069	0.250	0.212	1.16
	Na_e	4c	0	0.321	0.250	0.448	0.32
	Mn	4a	0	0	0	0.971	0.34
	Li	4a	0	0	0	0.029	0.34
	O	8f	0	0.662	0.093	1	5.00

Space group: *Cmcm*, a = 2.837 Å, b = 5.248 Å, c = 11.217 Å, α = β = γ= 90°, Vol = 166.995 Å^3, (Z = 4), *Rp* = 2.05%, R_{wp} = 2.97%， χ^2 = 3.168. g: occupancy. x, y, z: atomic coordinate.

Table S3. Rietveld refinement results for P′2-$Na_{0.67}Li_{0.05}Mn_{0.95}O_2$.

Sample	Atom	Site	x	y	z	g	B_{iso}
	Na_f	4c	0	-0.089	0.250	0.230	0.78
	Na_e	4c	0	0.318	0.250	0.425	0.50
$Na_{0.67}Li_{0.05}Mn_{0.95}O_2$	Mn	4a	0	0	0	0.945	0.42
	Li	4a	0	0	0	0.055	0.42
	O	8f	0	0.668	0.0838	1	3.67

Space group: *Cmcm*, a = 2.841 Å, b = 5.252 Å, c = 11.195 Å, α = β = γ= 90°, Vol = 167.047 Å^3, (Z = 4), *Rp* = 2.23%, R_{wp} = 3.13%， χ^2 = 3.725. g: occupancy. x, y, z: atomic coordinate.

Table S4. Rietveld refinement results for P′2-$Na_{0.67}Li_{0.08}Mn_{0.92}O_2$.

Sample	Atom	Site	x	y	z	g	B_{iso}
	Na_f	4c	0	-0.092	0.250	0.252	0.60
	Na_e	4c	0	0.325	0.250	0.438	0.65
$Na_{0.67}Li_{0.08}Mn_{0.92}O_2$	Mn	4a	0	0	0	0.920	0.46
	Li	4a	0	0	0	0.080	0.46
	O	8f	0	0.667	0.0837	1	3.83

Space group: *Cmcm*, a = 2.856 Å, b = 5.128 Å, c = 11.216 Å, α = β = γ= 90°, Vol = 164.270 Å^3, (Z = 4), *Rp* = 2.30%, R_{wp} = 3.37%， χ^2 = 4.040. g: occupancy. x, y, z: atomic coordinate.

Table S5. Lengths of Mn-O, MnO_2 layers thickness, Na interlayer spacing and interslab distance for P′2-$Na_{0.67}MnO_2$ and P′2-$Na_{0.67}Li_{0.05}Mn_{0.95}O_2$.

Sample	Mn-O (Å)	Mn-O' (Å)	MnO_2 (Å)	O-Na-O (Å)	Interslab distance (Å)
$Na_{0.67}MnO_2$	2.133	1.955	2.187	3.418	5.586
$Na_{0.67}Li_{0.05}Mn_{0.95}O_2$	1.980	1.917	1.877	3.721	5.598

Table S6. ICP-OES results for P′2-$Na_{0.67}MnO_2$ and P′2-$Na_{0.67}Li_{0.05}Mn_{0.95}O_2$.

Sample	Na	Li	Mn
$Na_{0.67}MnO_2$	0.659	0	1
$Na_{0.67}Li_{0.05}Mn_{0.95}O_2$	0.655	0.0557	0.944

Table S7. Structural parameters of OP4-type phase electrode cycled at 4.3 V during 2nd charge based on Rietveld refinement.

Sample	a	b	c	$d_{(Mn-O)}$
Na_xMnO_2	2.866	2.866	21.058	1.944
$Na_xLi_{0.05}Mn_{0.95}O_2$	2.840	2.840	20.820	1.928

Na_xMnO_2. Space group: *P63/ m m c* , α = β =90, γ= 120°, Vol = 149.82 Å^3, *Rp* = 2.40%, R_{wp} = 7.10%; $Na_xLi_{0.05}Mn_{0.95}O_2$. Space group: *P63/ m m c* , α = β =90, γ= 120°, Vol = 145.38 Å^3, *Rp* = 3.61%, R_{wp} = 8.49%.

Table S8. Structural parameters of P″2-type phase electrode cycled at 1.8 V during 1st discharge based on Rietveld refinement.

Sample	a	b	c	V	δ	$d_{(Mn-O)}$	$d'_{(Mn-O)}$
Na_xMnO	2.863	5.622	10.802	173.849	13.37%	2.305	1.890
$Na_xLi_{0.05}Mn_{0.95}O_2$	2.865	5.424	10.887	169.179	9.30%	2.230	1.854

Na_xMnO_2. Space group: *Cmcm*, α = β = γ= 90°, Vol = 173.849 Å^3, *Rp* = 2.51%, R_{wp} = 5.08%; $Na_xLi_{0.05}Mn_{0.95}O_2$. Space group: *Cmcm*, α = β = γ= 90°, Vol = 169.179 Å^3, *Rp* = 2.88%, R_{wp} = 6.57%.

Table S9. Summary of COHP analysis of Mn sites in P′2-$Na_{0.67}MnO_2$ and P′2-$Na_{0.67}Li_{0.05}Mn_{0.95}O_2$.

-COHP(avg)	Mn-O21	Mn-O22	Mn-O25	Mn-O26	Mn-O29	Mn-O35	Sum.
$Na_{0.67}MnO$	1.328	1.320	0.520	0.484	1.177	1.103	5.934
$Na_{0.67}Li_{0.05}Mn_{0.95}O_2$	1.408	1.460	1.266	1.190	1.131	1.217	7.673

References

1. L. Wang, C. Wang, N. Zhang, F. Li, F. Cheng and J. Chen, *ACS Energy Lett*. 2017, **2**, 256.
2. Y. Xiao, Y.-F. Zhu, H.-R. Yao, P.-F. Wang, X.-D. Zhang, H. Li, X. Yang, L. Gu, Y.-C. Li, T. Wang, Y.-X. Yin, X.-D. Guo, B.-H. Zhang, Y.-G. Guo, *Adv. Energy Mater*. 2019, **19**, 1803978.
3. G. Kresse, *Phys. Rev. B*. 1993, **47**, 558.
4. G. Kresse and J. Furthmüller, *Phys. Rev. B*. 1996, **54**, 11169.
5. J. P. Perdew and Y. Wang, *Phys. Rev. B*. 1992, **45**, 13244.
6. S. L. Dudarev, G. A. Botton, S. Y. Savrasov, C. J. Humphreys and A. P. Sutton, *Phys. Rev. B*. 1998, **57**, 1505.

7. Y. J. Park, J. U. Choi, J. H. Jo, C.-H. Jo, J. Kim and S.-T. Myung, *Adv. Funct. Mater*. 2019, **29**, 1901912.
8. R. Dronskowski and P. E. Bloechl, *J. Phys. Chem*. 1993, **97**, 8617.
9. S. Maintz, V. L. Deringer, A. L. Tchougréeff and R. Dronskowski, *J. Comput. Chem*. 2016, **37**, 1030.
10. G. Henkelman, B. P. Uberuaga and H. Jónsson, *J. Chem. Phys*. 2000, **113**, 9901.